

# Energy dependence of transverse mass spectra of kaons produced in p+p and p+ $\bar{p}$ interactions. A compilation.

Michael Kliemant<sup>a</sup>, Benjamin Lungwitz<sup>a</sup>  
and Marek Gaździcki<sup>a,b</sup>

August 20, 2005

<sup>a</sup> Institut für Kernphysik, Universität Frankfurt, Germany

<sup>b</sup> Świętokrzyska Academy, Kielce, Poland

## Abstract

The data on  $m_T$  spectra of  $K_S^0$ ,  $K^+$  and  $K^-$  mesons produced in all inelastic p+p and p+ $\bar{p}$  interactions in the energy range  $\sqrt{s_{NN}} = 4.7 - 1800$  GeV are compiled and analyzed. The spectra are parameterized by a single exponential function,  $\frac{dN}{m_T dm_T} = C \cdot e^{-m_T/T}$ , and the inverse slope parameter  $T$  is the main object of study. The  $T$  parameter is found to be similar for  $K_S^0$ ,  $K^+$  and  $K^-$  mesons. It increases monotonically with collision energy from  $T \approx 130$  MeV at  $\sqrt{s_{NN}} = 4.7$  GeV to  $T \approx 220$  MeV at  $\sqrt{s_{NN}} = 1800$  GeV. The  $T$  parameter measured in p+p( $\bar{p}$ ) interactions is significantly lower than the corresponding parameter obtained for central Pb+Pb collisions at all studied energies. Also the shape of the energy dependence of  $T$  is different for central Pb+Pb collisions and p+p( $\bar{p}$ ) interactions.

## 1 Introduction

The search for signals of the deconfinement phase transition and thus evidence for the existence of a quark gluon plasma in nature was the main objective of the experimental study of nucleus–nucleus (A+A) collisions at high energies.

Recent results obtained in broad range of energy allowed to identify anomalies in the energy dependence of hadron production in central Pb+Pb collisions [1, 2]. They suggest that, in fact, the onset of deconfinement is observed and is located at the low CERN SPS energies  $\sqrt{s_{NN}} \approx 7.5$  GeV [3, 4]. Among basic observables used in this study are pion and kaon multiplicities and transverse mass spectra of kaons. In the identification of the effects related to the onset of deconfinement in A+A collisions a comparison with the corresponding results obtained in nucleon-nucleon (N+N) interactions plays a special role. In case of the study of energy dependence of pion and kaon multiplicities this comparison was done based on the existing compilations of the data on all inelastic proton-proton (p+p), proton-neutron (p+n) and proton-antiproton (p+ $\bar{p}$ ) interactions [5, 6].

A recently found [4] anomaly in the energy dependence of the shape of transverse mass spectra of kaons produced in central Pb+Pb collisions raised already significant interest [7, 8, 9, 10, 11]. However, the results on transverse mass spectra of kaons in N+N interactions were up to now not compiled and a detailed comparison with the corresponding A+A data was missing. The aim of our paper is to fill this gap.

The paper is organized as follows. In section 2 the existing data are reviewed and analyzed. The energy dependence of the spectra is presented and discussed in section 3. The paper is closed by the summary, section 4.

## 2 A compilation of p+p( $\bar{p}$ ) data

Most of the results on kaon transverse momentum ( $p_T$ ) spectra in all inelastic p+p( $\bar{p}$ ) interactions are obtained for  $K_S^0$  mesons and we start our compilation from the review and analysis of these data. Further on we compile and analyze data on charged kaon ( $K^+$ ,  $K^-$ ) production.

In most cases the original experimental papers present  $p_T$  spectra in the form  $\frac{d^3n}{dp_T^2 dy}$  or  $\frac{Ed^3n}{d\vec{p}}$ . From these results the transverse mass  $m_T$  ( $m_T = \sqrt{p_T^2 + m_0^2}$ , where  $m_0$  is the particle rest mass) spectra  $\frac{d^2n}{m_T dm_T dy}$  can be easily obtained ( $\frac{d^2n}{m_T dm_T dy} \sim \frac{d^3n}{dp_T^2 dy} \sim \frac{Ed^3n}{d\vec{p}}$ ).

Our compilation and analysis is limited to the low  $p_T$  region,  $p_T \leq 1.3$  GeV/c. First, it is because in this region the energy dependence of the  $m_T$  spectrum of kaons produced in A+A collisions was studied. Second, only in this region an exponential parameterization of the p+p( $\bar{p}$ ) data as used

for the analysis of A+A collisions [1, 2]

$$\frac{dn}{m_T dm_T} = C \cdot e^{-m_T/T} \quad (1)$$

is approximately valid <sup>1</sup>. In Eq. 1 the inverse slope parameter  $T$  and the normalization parameter  $C$  are treated as free parameters and their values are extracted from the least square fits to the experimental spectra.

The compiled  $p_T$  spectra are measured either at midrapidity ( $y \approx 0$ ) or they are integrated over forward or backward hemispheres starting from midrapidity. The rapidity of kaons peaks at midrapidity [21-29] and thus the shape of the integrated spectra is dominated by the contribution from this region. In the following we do not distinguish between both types of measurements.

## 2.1 $K_S^0$ spectra

Transverse momentum spectra of  $K_S^0$  mesons produced in all inelastic p+p interactions [21-29] are measured in fixed target, mostly bubble chamber experiments, at energies below  $\sqrt{s_{NN}} \approx 30$  GeV. At higher energies,  $\sqrt{s_{NN}} = 200 - 900$  GeV, the measurements for p+ $\bar{p}$  interactions are performed at the Sp $\bar{p}$ S collider [30, 31]. The  $K_S^0$  data come from the analysis of charged decays of  $K_S^0$  mesons,  $K_S^0 \rightarrow \pi^+ + \pi^-$ . A characteristic feature of these results are relatively low systematic uncertainties and large statistical errors due to the small number of analyzed events.

The summary of the data on  $m_T$  spectra of  $K_S^0$  mesons is given in Tables 1 and 2, where  $\sqrt{s_{NN}}$ , the  $p_T$  range selected for the analysis, the rapidity ( $y$ ) range in which the measurement was done and the reference to the original experimental papers are given. The  $m_T$  spectra are plotted as a function of  $m_T - m_0$  in Fig. 1. The normalization of the spectra is arbitrary. They are ordered from bottom to top according to increasing energy.

The spectra displayed in Fig. 1 are fitted by an exponential function, Eq. 1, in the whole  $m_T$  range ( $m_T - m_0 \leq 0.85$  GeV/ $c^2$ ) as well as in two subintervals, the “low- $m_T$ ” interval ( $m_T - m_0 \leq 0.25$  GeV/ $c^2$ ) and the “high- $m_T$ ” interval ( $0.25 < m_T - m_0 \leq 0.85$  GeV/ $c^2$ ). The inverse slope parameter  $T$  and  $\chi^2/NDF$  resulting from the fits in the whole interval are given in Tables 1 and 2. The corresponding functions are plotted in Fig. 1 by solid lines. It is seen that the used parametrization (Eq. 1), reasonably well describes  $K_S^0$  spectra in the whole  $m_T$  range at all studied energies

<sup>1</sup>At high  $m_T$  the spectra obey a power law behavior,  $\frac{dn}{m_T dm_T} \sim m_T^{-P}$ , which is interpreted as due to hard (parton) scattering.

( $\sqrt{s_{NN}} = 4.7 - 900$  GeV), both for p+p and p+ $\bar{p}$  interactions. Differences observed between results obtained for “low- $m_T$ ” and “high- $m_T$ ” intervals are shown and discussed in section 3.

## 2.2 $K^+$ and $K^-$ spectra

A summary of the data used in the analysis of the  $m_T$  spectra of  $K^+$  and  $K^-$  mesons produced in p+p interactions at the ISR [33] and fixed target experiments [32, 34] is given in Tables 3 and 4. In Table 5 the data on charged kaon spectra in p+ $\bar{p}$  interactions at the Sp $\bar{p}$ S [36] and the Tevatron [20, 35] are compiled. In most cases the  $K^+$  and  $K^-$  identification is done by means of time of flight [20, 33] and energy loss measurements [32] or by use of gas Cerenkov counters [33]. In the bubble chamber experiment [34] the kaons were identified by the analysis of their decays.

The  $m_T$  spectra of  $K^+$  and  $K^-$  mesons are plotted in Figs. 2 and 3 together with the exponential functions (Eq. 1) fitted in the whole  $m_T$  interval. The corresponding  $T$  parameter and  $\chi^2/NDF$  are given in Tables 3, 4 and 5. Majority of the  $K^+$  and  $K^-$  spectra follow reasonably well the parametrization. The most significant deviations are observed for the  $K^+$  spectra at  $\sqrt{s_{NN}} = 63$  GeV and the  $K^-$  spectra at  $\sqrt{s_{NN}} = 53$  and 63 GeV. The results obtained for the fits in “low- $m_T$ ” and “high- $m_T$ ” intervals, which allow to quantify the observed deviations, are shown and discussed in section 3.

## 3 The energy dependence

### 3.1 Results

The energy dependence of the  $T$  parameter fitted in the whole  $m_T$  interval ( $m_T - m_0 \leq 0.85$  GeV/ $c^2$ ) to the  $m_T$  spectra of kaons produced in all inelastic p+p( $\bar{p}$ ) interactions is shown in Fig. 4. No significant differences are seen between results obtained for  $K_S^0$ ,  $K^+$  and  $K^-$  mesons as well as between data for p+p and p+ $\bar{p}$  interactions.

The dependence of the  $T$  parameter on  $\sqrt{s_{NN}}$  was fitted by an expression:

$$T = a + b \cdot \ln \sqrt{s_{NN}}, \quad (2)$$

where  $a$  and  $b$  are fit parameters and  $\sqrt{s_{NN}}$  is given in units of GeV. The best fit to the data presented in Fig. 4 yields  $a = (115 \pm 2.8)$  MeV,  $b = (13.7 \pm 0.7)$  MeV and  $\chi^2/NDF = 120/30$ . For most of the points the observed spread around the parameterization is consistent with one expected from statistical fluctuations. Only the points at  $\sqrt{s_{NN}} = 23.7$  GeV [26],  $\sqrt{s_{NN}} = 540$  GeV

[35] and  $\sqrt{s_{NN}} = 900$  GeV [30] deviate by more than 3 standard deviations. The compiled results indicate that  $T$  increases monotonically with collision energy from  $T \approx 130$  MeV at  $\sqrt{s_{NN}} = 4.7$  to  $T \approx 220$  MeV at 1800 GeV.

The inverse slope parameters obtained from the fits performed in the “low- $m_T$ ” and “high- $m_T$ ” intervals are plotted as a function of collision energy in Fig. 5. Up to  $\sqrt{s_{NN}} \approx 20$  GeV the  $T$  values for the “low- $m_T$ ” and “high- $m_T$ ” intervals are approximately equal. At higher energies the  $T$  parameter for “low- $m_T$ ” interval is systematically lower than for the “high- $m_T$ ” interval. For the “low- $m_T$ ” interval the  $T$  parameter is approximately independent of the collision energy, whereas in the “high- $m_T$ ” interval it seems to increase. The observed behaviour may be attributed to rapid development of the power law tail with increasing collision energy.

The data on the  $T$  parameter were fitted by the logarithmic function, Eq. 2, for each interval separately. The resulting parameters and  $\chi^2/NDF$  are:  $a = (139 \pm 7.7)$  MeV,  $b = (-0.1 \pm 2.2)$  MeV,  $\chi^2/NDF = 39/24$  and  $a = (110 \pm 7)$  MeV,  $b = (18.2 \pm 1.7)$  MeV,  $\chi^2/NDF = 60/24$  for “low- $m_T$ ” and “high- $m_T$ ” intervals, respectively. The functions fitted in both subintervals and the whole  $m_T$  interval are shown in Fig. 5 for a comparison.

In Figs. 6 and 7 the results on the  $T$  parameter of kaons obtained for p+p( $\bar{p}$ ) interactions are plotted as a function of  $\sqrt{s_{NN}}$  together with the corresponding data for central Pb+Pb (Au+Au) collisions at AGS [12], SPS [1, 2] and RHIC [13, 14]. The data points for central Pb+Pb (Au+Au) collisions and p+p( $\bar{p}$ ) interactions were extracted from the fits performed in the whole  $m_T$  interval. A different dependence is measured in Pb+Pb (Au+Au) collisions than in p+p( $\bar{p}$ ) interactions. At all energies the  $T$  parameter is significantly higher in Pb+Pb (Au+Au) collisions than in elementary interactions. In the case of heavy ion collisions a well developed plateau at SPS energies is observed. There is no obvious sign of such behaviour for p+p( $\bar{p}$ ) interactions, however, the precision of these data is low and they can not exclude anomalies similar to this observed for Pb+Pb (Au+Au) collisions.

## 3.2 Discussion

The compilation of the p+p( $\bar{p}$ ) data performed in this paper was triggered by the observation of the anomalous energy dependence of the shape of transverse mass spectra of kaons measured in central Pb+Pb (Au+Au) collisions and its possible relation to the deconfinement phase transition [4]. Within statistical-hydrodynamic approach to A+A collisions the heavy ion data shown in Fig. 6 are interpreted as follows.

The  $T$  parameter increases strongly with collision energy up to the lowest CERN SPS energies ( $\sqrt{s_{NN}} \approx 7$  GeV). This is an energy region where the

creation of confined matter at the early stage of the collisions is expected. Increasing collision energy leads to an increase of the early stage temperature and pressure. This results in grow of the transverse collective flow velocity,  $\bar{v}_T$ , and temperature  $T_f$ , at freeze-out. Consequently the transverse activity of produced hadrons, measured by the inverse slope parameter, increases with increasing energy.

The  $T$  parameter is approximately independent of the collision energy in the SPS energy range,  $\sqrt{s_{NN}} = 7 - 20$  GeV. In this energy region the transition between confined and deconfined matter is expected to be located. The resulting modification of the equation of state “suppresses” an increase of both  $T_f$  and  $\bar{v}_T$ , and this leads to the observed plateau structure in the energy dependence of the  $T$  parameter.

At RHIC ( $\sqrt{s_{NN}} = 130$  GeV and 200 GeV) the  $T$  is significantly larger than at SPS energies. In the RHIC energy domain the equation of state at the early stage becomes again stiff, the early stage temperature and pressure increase with collision energy. This results in increase of the transverse flow  $\bar{v}_T$  and, consequently, in increase of  $T$  between SPS and RHIC energies.

Within the above picture there are two basic differences between central collisions of heavy nuclei and p+p interactions.

First, collective expansion effects are expected to be important only in heavy ion collisions, as they result from the pressure gradient generated in the dense interacting matter. The expansion leads to an increase of the  $T$  parameter and consequently one predicts a lower values of  $T$  in p+p interactions, where collective expansion is absent and hadrons are emitted directly from the fragmentation of strings, than in central A+A collisions. This qualitative prediction is independent of the state of matter created at the early stage of the collisions and thus it is valid at all collision energies. In fact, it is confirmed by the data compiled in this paper (see Fig. 6).

Second, the stationary value of  $T$  at SPS energies is related to the modification of the equation of state of matter created at the early stage for mixed phase and thus relative suppression of the collective expansion. As the collective expansion is absent in p+p interactions and, in general, the applicability of statistical models is in question for elementary interactions, one does not expect to observe any anomaly in energy dependence of  $T$  in p+p interactions. This prediction is not in contradiction with the data compiled in this paper. However, large experimental errors allow to exclude only relatively large effects.

The string hadronic models (Fritiof [15], UrQMD [16], HSD [17, 18]) well describe results on  $T$  for p+p interactions [9]. Models without rescattering (see e.g. Fritiof [15]) predict similar values of  $T$  for p+p interactions and central A+A collisions. These approaches are obviously excluded by the

data. The models with rescattering of initially produced strings and hadrons should, in general, lead to an increase of  $T$  for central A+A collisions. Surprisingly, it was recently found [9] within HSD and UrQMD models, that the rescattering only weakly influences shape of the transverse mass spectra of kaons. Thus also these approaches significantly under-predict the  $T$  parameter measured in central A+A collisions at all energies [9].

Within microscopic picture of A+A collisions one may try to speculate whether a part of the observed increase of  $T$  when going from p+p interactions to central A+A collisions is related to the higher excitation of nucleons in A+A collisions than in all inelastic interactions. The experimental results, which can shed light on this subject are poor, but nevertheless, at collision energies up to top SPS energy they seem to contradict this hypothesis. Relatively rich data on pion production in p+p interactions as a function of multiplicity of produced hadrons show that the mean transverse momentum (and the  $T$  parameter) decreases with increasing multiplicity [19]. Independence of the shape of  $p_T$  spectrum of kaons on multiplicity is suggested by the p+p results at 12-200 GeV [22]. One should note, however, that at Tevatron energies an increase of  $\langle p_T \rangle$  of pions and kaons with multiplicity is observed [20].

## 4 Summary

We compiled and analyzed data on  $m_T$  spectra of  $K_S^0$ ,  $K^+$  and  $K^-$  mesons produced in all inelastic p+p and p+ $\bar{p}$  interactions. The spectra can be reasonably well described by a simple exponential parametrization  $\frac{dN}{m_T dm_T} = C \cdot e^{-m_T/T}$  in the whole analyzed  $m_T$  interval ( $m_T - m_0 \leq 0.85 \text{ GeV}/c^2$ ). The values of the parameter  $T$  measured for  $K_S^0$ ,  $K^+$  and  $K^-$  are similar. We do not observe any significant difference between data from p+p and p+ $\bar{p}$  interactions. The  $T$  parameter increases monotonically with  $\sqrt{s_{NN}}$  from  $T \approx 130 \text{ MeV}$  at  $\sqrt{s_{NN}} = 4.7 \text{ GeV}$  to  $T \approx 220 \text{ MeV}$  at  $\sqrt{s_{NN}} \approx 1800 \text{ GeV}$ . This dependence can be parametrized as  $T = (115 \pm 2.9) \text{ MeV} + (13.7 \pm 0.7) \text{ MeV} \cdot \ln(\sqrt{s_{NN}})$ , where  $\sqrt{s_{NN}}$  is given in units of GeV. The  $T$  measured in p+p ( $\bar{p}$ ) is significantly lower than the corresponding measurement in Pb+Pb (Au+Au) collisions. Also the shape of the energy dependence of  $T$  on energy is different for central Pb+Pb collisions and p+p( $\bar{p}$ ) interactions.

**Acknowledgments.** We thank Rainer Renfordt for reading and commenting our work and our colleagues at IKF and Marco van Leeuwen (NIKHEF) for discussions and comments. Partial support by Bundesministerium für Bildung und Forschung and by Polish Committee of Scientific Research under

grant 2P03B04123 (M. G.) is acknowledged.

## References

- [1] S. V. Afanasiev *et al.* [NA49 Collaboration], Phys. Rev. C **66**, 054902 (2002) [arXiv:nucl-ex/0205002].
- [2] C. Alt *et al.* [NA49 Collaboration], arXiv:nucl-ex/0305017.
- [3] M. Gazdzicki and M. I. Gorenstein, Acta Phys. Polon. B **30**, 2705 (1999) [arXiv:hep-ph/9803462].
- [4] M. I. Gorenstein, M. Gazdzicki and K. A. Bugaev, Phys. Lett. B **567**, 175 (2003) [arXiv:hep-ph/0303041].
- [5] M. Gazdzicki and D. Roehrich, Z. Phys. C **65**, 215 (1995).
- [6] M. Gazdzicki and D. Rohrich, Z. Phys. C **71**, 55 (1996) [arXiv:hep-ex/9607004].
- [7] B. Mohanty, arXiv:nucl-th/0307086.
- [8] B. Mohanty, J. e. Alam, S. Sarkar, T. K. Nayak and B. K. Nandi, arXiv:nucl-th/0304023.
- [9] E. L. Bratkovskaya, S. Soff, H. Stoecker, M. van Leeuwen and W. Cassing, arXiv:nucl-th/0307098.
- [10] M. Gazdzicki, M. I. Gorenstein, F. Grassi, Y. Hama, T. Kodama and O. Socolowski, arXiv:hep-ph/0309192.
- [11] F. Grassi, Y. Hama, T. Kodama and O. Socolowski, arXiv:hep-ph/0307306.
- [12] L. Ahle *et al.* [E866 Collaboration], Phys. Lett. B **490**, 53 (2000) [arXiv:nucl-ex/0008010].
- [13] D. Ouerdane [BRAHMS Collaboration], Nucl. Phys. A **715**, 478 (2003) [arXiv:nucl-ex/0212001].
- [14] C. Adler *et al.* [STAR Collaboration], arXiv:nucl-ex/0206008.
- [15] B. Andersson, G. Gustafson and H. Pi, Z. Phys. C **57**, 485 (1993).
- [16] M. Bleicher *et al.*, J. Phys. G **25**, 1859 (1999) [arXiv:hep-ph/9909407].



- [17] J. Geiss, W. Cassing and C. Greiner, Nucl. Phys. A **644**, 107 (1998) [arXiv:nucl-th/9805012].
- [18] W. Cassing and E. L. Bratkovskaya, Phys. Rept. **308**, 65 (1999).
- [19] A. I. Golokhvastov, JINR-P2-2002-92
- [20] T. Alexopoulos *et al.* [E0735 Collaboration], Phys. Rev. Lett. **64**, 991 (1990).
- [21] V. Blobel *et al.* [Bonn-Hamburg-Munich Collaboration], Nucl. Phys. B **69**, 454 (1974).
- [22] K. Jaeger, D. Colley, L. Hyman and J. Rest, Phys. Rev. D **11**, 2405 (1975).
- [23] V. V. Ammosov *et al.*, Nucl. Phys. B **115**, 269 (1976).
- [24] J. W. Chapman *et al.*, Phys. Lett. B **47**, 465 (1973).
- [25] D. Brick *et al.*, Nucl. Phys. B **164**, 1 (1980).
- [26] F. Lopinto *et al.*, Phys. Rev. D **22**, 573 (1980).
- [27] A. Sheng *et al.*, Phys. Rev. D **11**, 1733 (1975).
- [28] M. Asai *et al.* [EHS-RCBC Collaboration], Z. Phys. C **27**, 11 (1985).
- [29] H. Kichimi *et al.*, Phys. Rev. D **20**, 37 (1979).
- [30] R. E. Ansorge *et al.*, Z. Phys. C **41**, 179 (1988).
- [31] G. Bocquet *et al.* [UA1 Collaboration], Phys. Lett. B **366**, 441 (1996).
- [32] I. Kraus [NA49 Collaboration], arXiv:nucl-ex/0306022.
- [33] B. Alper *et al.* [British-Scandinavian Collaboration], Nucl. Phys. B **100**, 237 (1975).
- [34] E. E. Zabrodin *et al.*, Phys. Rev. D **52**, 1316 (1995).
- [35] T. Alexopoulos *et al.* [Fnl-735 Experiment], Phys. Rev. D **48**, 984 (1993).
- [36] M. Banner *et al.* [UA2 Collaboration], Phys. Lett. B **122**, 322 (1983).

Table 1: Summary of the data on the  $p_T$  spectra of  $K_S^0$  produced in p+p interactions. The collision energy  $\sqrt{s_{NN}}$ , the  $p_T$ -range used for the analysis, the c. m. rapidity range in which  $p_T$  spectrum was measured and the references to the original papers are given. The fitted inverse slope parameter  $T$  and  $\chi^2/NDF$  are also presented.

$\sqrt{s}$ (GeV)	$p_T$ -range(GeV/c)	y-range	$T$ (MeV)	$\chi^2/NDF$	ref.
4.74	0-1.025	0-2.0	$130.2 \pm 3.3$	8.2/6	[21]
4.82	0-0.906	0-1.7	$135.5 \pm 11.4$	0.45/4	[22]
6.7	0-1.025	0-2.0	$141.2 \pm 3.4$	14/6	[21]
11.4	0-0.945	0-2.4	$148.3 \pm 10.5$	2.4/8	[23]
13.8	0-0.951	0-2.0	$168.3 \pm 17.5$	1.4/4	[24]
16.6	0-0.897	0-0.6	$149.3 \pm 10.6$	18/4	[25]
19.6	0-0.889	0-3.0	$153.4 \pm 10.7$	1.2/6	[22]
23.7	0-1.225	0-3.0	$191.4 \pm 4.8$	17/6	[26]
23.7	0-0.787	-3.0-0	$156 \pm 14.3$	2.8/5	[27]
25.9	0-1.161	0-3.2	$152.7 \pm 5.9$	6.1/8	[28]
27.5	0-1.165	0-3.0	$169.4 \pm 8.1$	4.3/7	[29]

Table 2: Summary of the data on the  $p_T$  spectra of  $K_S^0$  produced in p+ $\bar{p}$  interactions. For details see the caption of Table 1.

$\sqrt{s}$ (GeV)	$p_T$ -range(GeV/c)	y-range	$T$ (MeV)	$\chi^2/NDF$	ref.
200	0.41-1.16	0-3.5	$183.9 \pm 23.2$	2.3/3	[30]
630	0.275-1.22	$ \eta  < 2.5$	$208 \pm 6.6$	35/11	[31]
900	0.38-1.17	0-3.5	$248.6 \pm 12.4$	4.2/4	[30]

Table 3: Summary of the data on the  $p_T$  spectra of  $K^+$  produced in p+p interactions. For details see the caption of Table 1.

$\sqrt{s}$ (GeV)	$p_T$ -range(GeV/c)	y-range	$T$ (MeV)	$\chi^2/NDF$	ref.
17.2	0-1.3	$y \approx 0$	$172 \pm 17$		[32]
23	0.1-1.2	$y \approx 0$	$161.5 \pm 4.9$	9.5/5	[33]
31	0.1-1.2	$y \approx 0$	$169.5 \pm 5.2$	8.3/5	[33]
45	0.1-1.2	$y \approx 0$	$155 \pm 4.9$	5/5	[33]
53	0.1-1.2	$y \approx 0$	$167.5 \pm 5.2$	23/5	[33]
63	0.1-1.2	$y \approx 0$	$179.4 \pm 13.8$	34/6	[33]

Table 4: Summary of the data on the  $p_T$  spectra of  $K^-$  produced in p+p interactions. For details see the caption of Table 1.

$\sqrt{s}$ (GeV)	$p_T$ -range(GeV/c)	y-range	$T$ (MeV)	$\chi^2/NDF$	ref.
7.74	0-1.025	$y \approx 0$	$146.9 \pm 41.1$	1.81/8	[34]
17.2	0-1.3	$y \approx 0$	$164 \pm 16$		[32]
23	0.1-1.2	$y \approx 0$	$150.7 \pm 5.1$	6.7/5	[33]
31	0.1-1.2	$y \approx 0$	$145.8 \pm 5.8$	11/5	[33]
45	0.1-1.2	$y \approx 0$	$161.8 \pm 6.2$	5.9/5	[33]
53	0.1-1.2	$y \approx 0$	$177.8 \pm 5.6$	33/5	[33]
63	0.1-1.2	$y \approx 0$	$185.6 \pm 13.9$	31/6	[33]

Table 5: Summary of the data on the  $p_T$  spectra of  $K^+ + K^-$  produced in p+ $\bar{p}$  interactions. For details see the caption of Table 1.

$\sqrt{s}$ (GeV)	$p_T$ -range(GeV/c)	y-range	$T$ (MeV)	$\chi^2/NDF$	ref.
300	0.28-1.22	$y \approx 0$	$192.6 \pm 9.8$	15.7/7	[35]
540	0.28-1.22	$y \approx 0$	$158.9 \pm 8.1$	11.2/7	[35]
540	0.45-1.05	$y \approx 0$	$215.7 \pm 18.4$	6.8/5	[36]
1000	0.28-1.22	$y \approx 0$	$217.8 \pm 6.7$	11.2/7	[35]
1800	0.28-1.17	$y \approx 0$	$213.1 \pm 5.1$	11/17	[20]

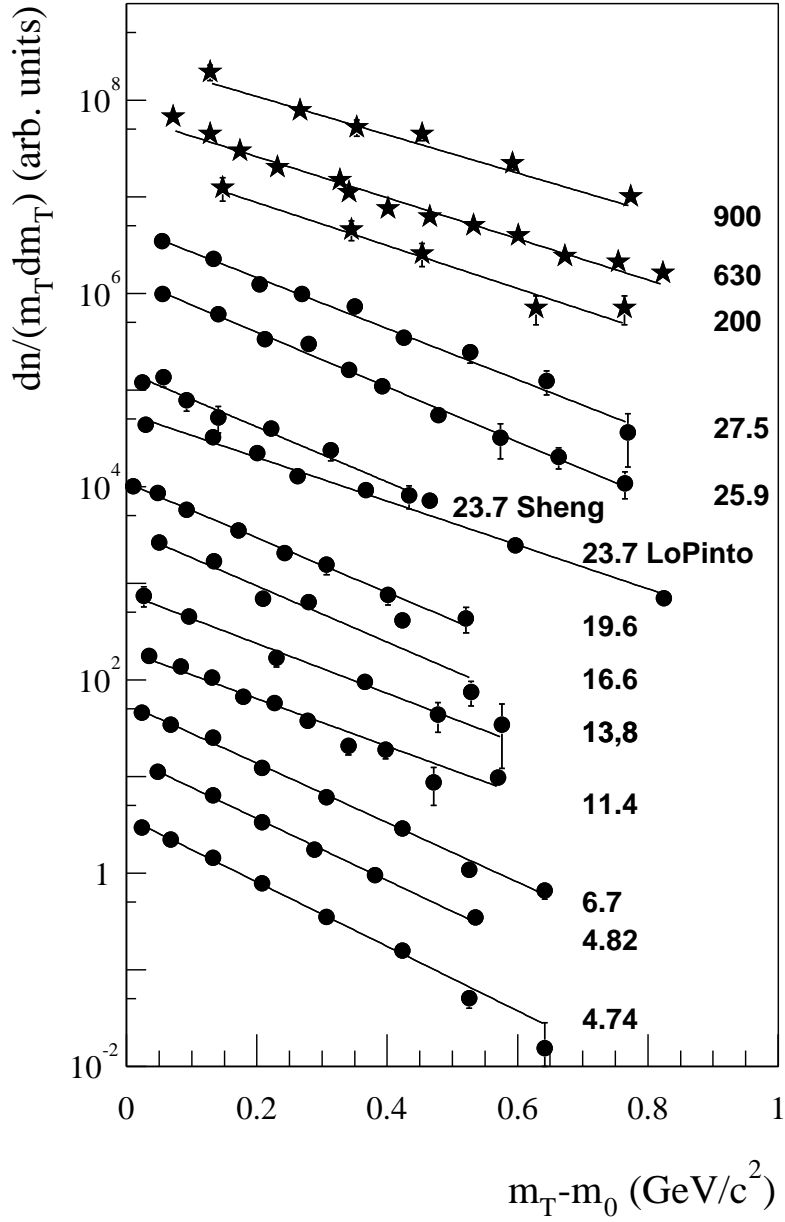


Figure 1: Transverse mass spectra of  $K_S^0$  mesons produced in p+p (circles) and p+p $\bar{p}$  (stars) interactions. The normalization of the spectra is arbitrary and the numbers next to the spectra give c. m. collision energy in GeV. The fits of the exponential function (Eq. 1) are indicated by the solid lines.

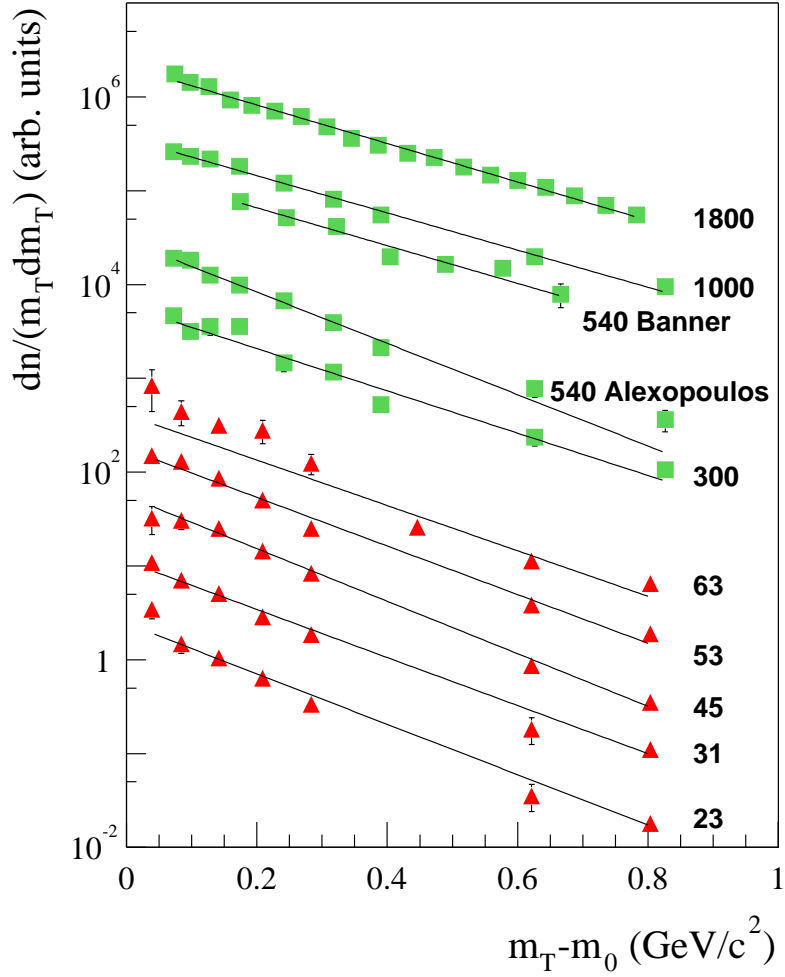


Figure 2: (Color online) Transverse mass spectra of  $K^+$  mesons produced in  $p+p$  interactions (triangles) and  $K^+K^-$  mesons produced in  $p+\bar{p}$  interactions (squares). For details see the caption of Fig. 1.

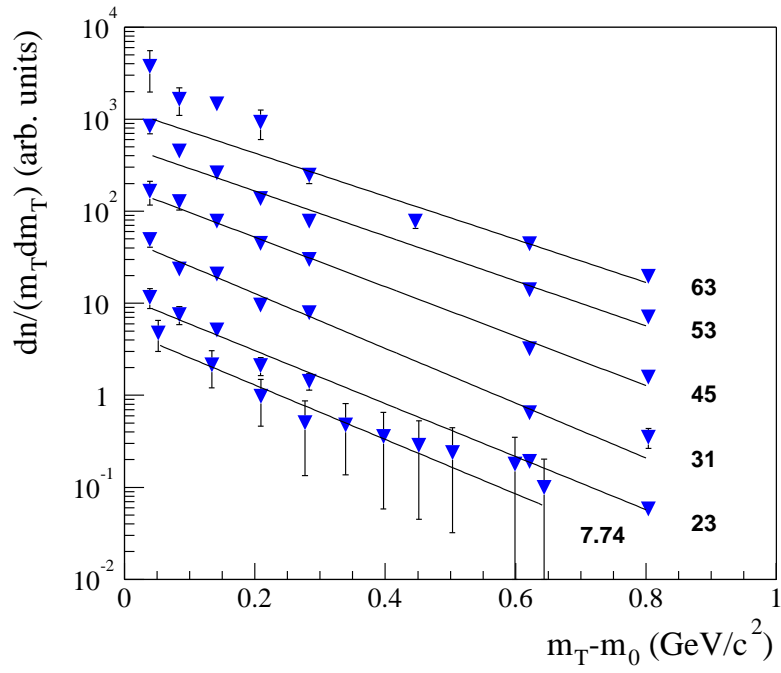


Figure 3: (Color online) Transverse mass spectra of  $K^-$  mesons produced in p+p interactions. For details see the caption of Fig. 1.

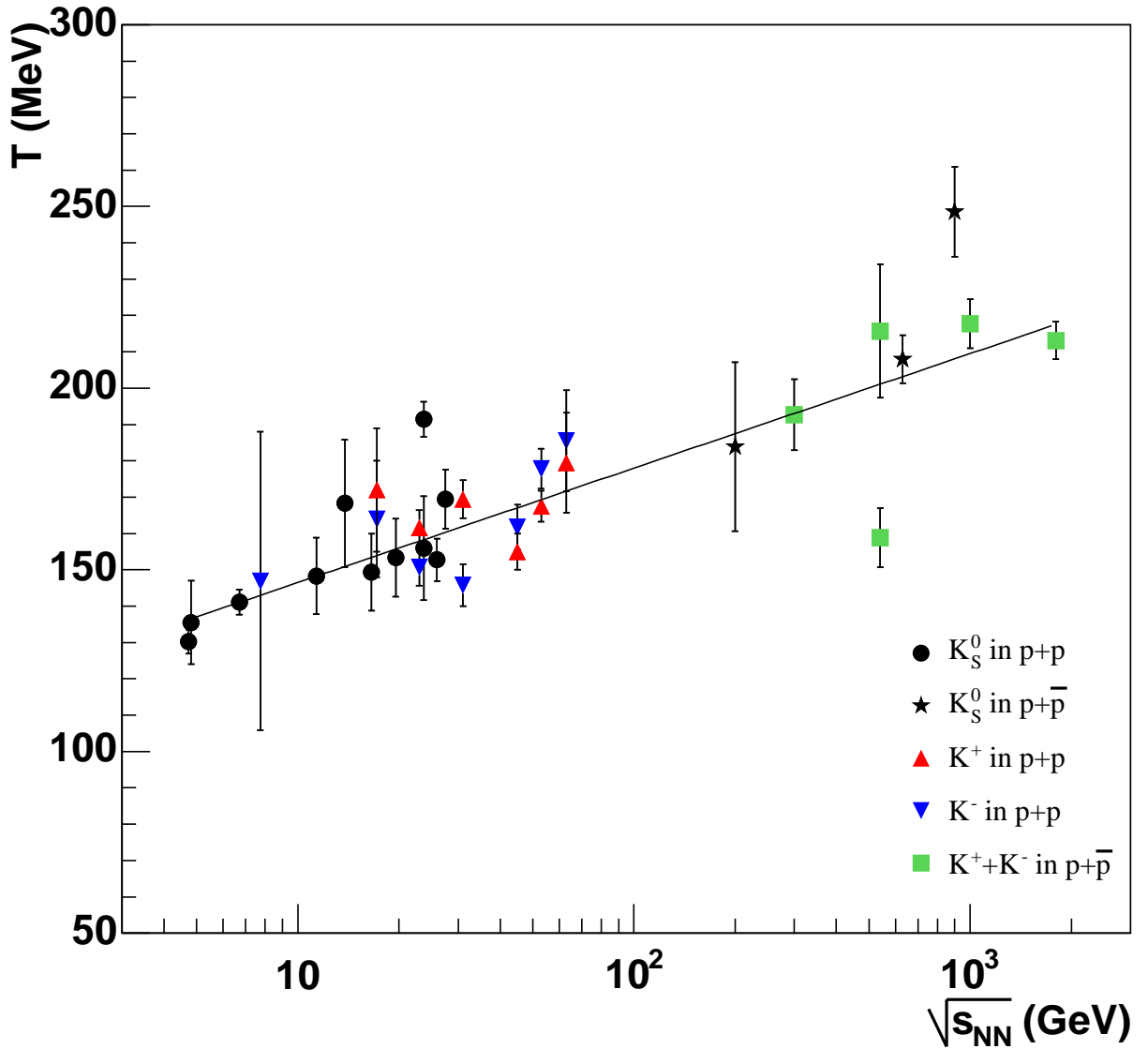


Figure 4: (Color online) Energy dependence of the inverse slope parameter  $T$  of transverse mass spectra of  $K_S^0$ ,  $K^+$  and  $K^-$  mesons produced in p+p and p+p-bar interactions. The  $T$  parameter was determined by fitting the spectra (Eq. 1) in the whole analyzed  $m_T$  interval,  $m_T - m_0 < 0.25$  GeV/ $c^2$ . The logarithmic parameterization is indicated by solid line.

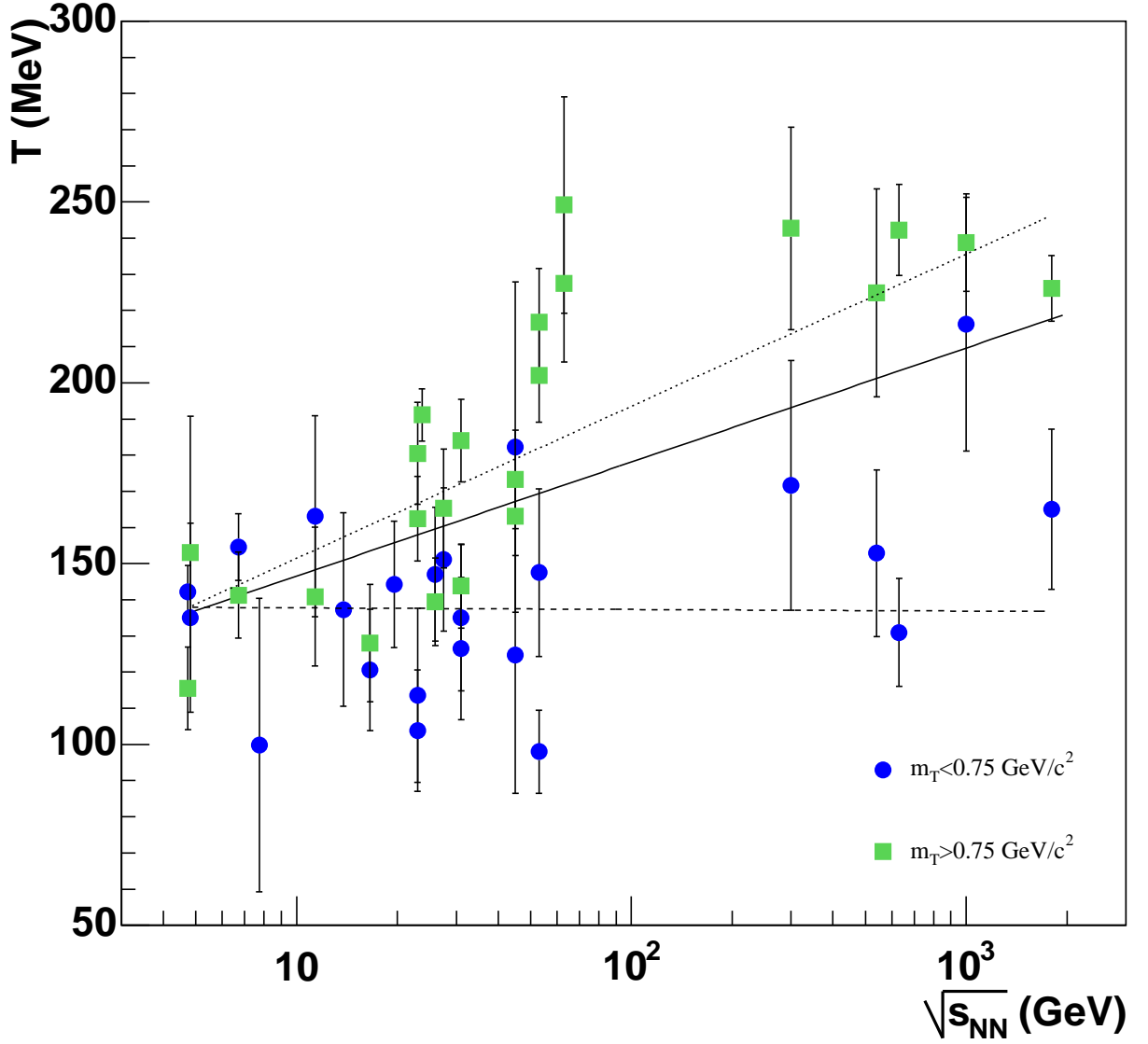


Figure 5: (Color online) Energy dependence of the inverse slope parameter  $T$  of transverse mass spectra of  $K_S^0$ ,  $K^+$  and  $K^-$  mesons produced in p+p and p+ $\bar{p}$  interactions, fitted separately in the “high” and “low”  $m_T$  intervals. The dashed and dotted lines show parameterizations of data for “low” and “high”  $m_T$  intervals, respectively. The parameterization obtained for the whole  $m_T$  interval is indicated by a solid line for comparison. Points with errors larger than 50 MeV are not plotted.



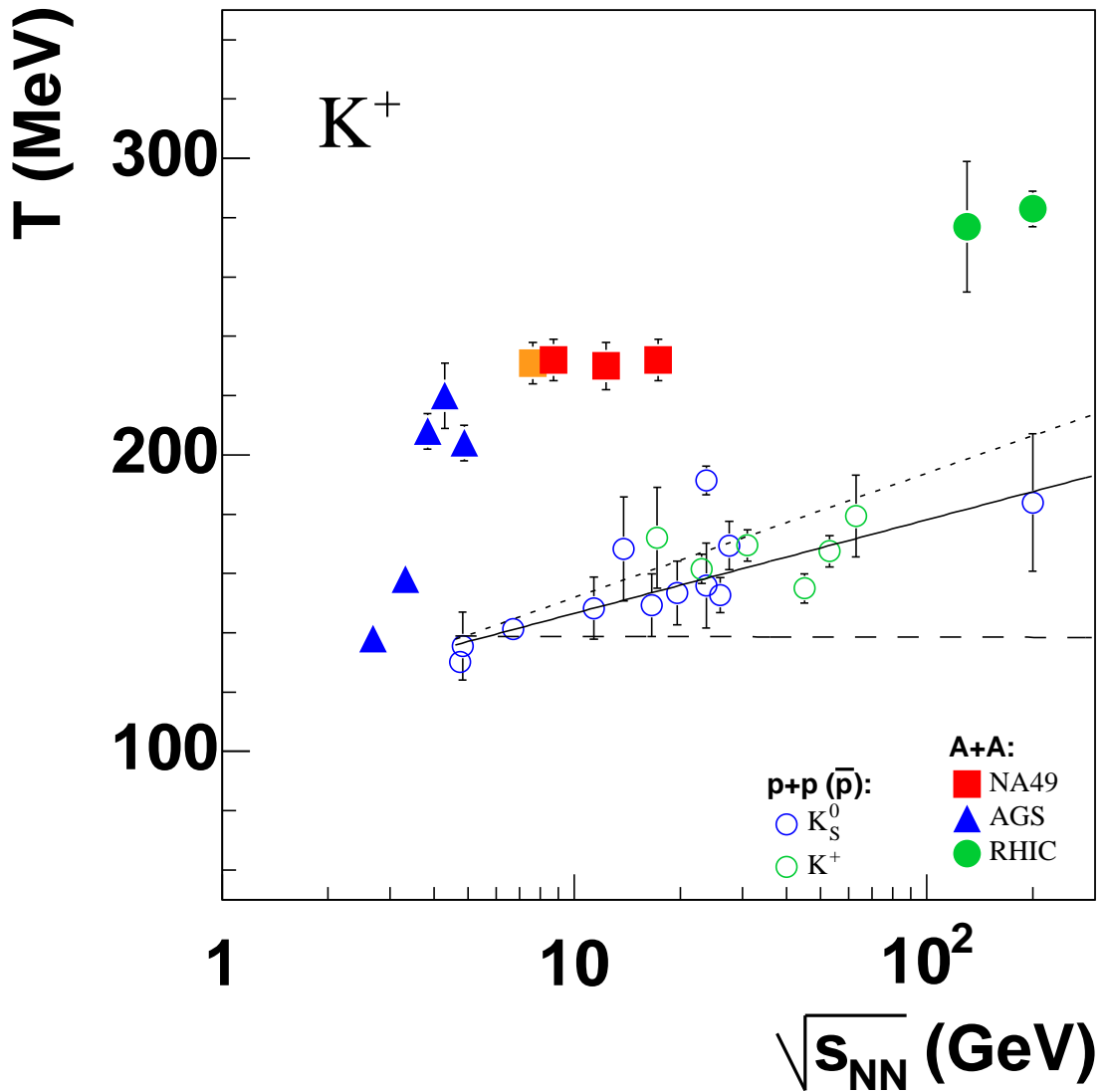


Figure 6: (Color online) Energy dependence of the inverse slope parameter  $T$  of transverse mass spectra of  $K^+$  mesons produced in central collisions of heavy nuclei (Pb+Pb [1, 2], Au+Au [12, 13, 14]) as well as  $K^+$  and  $K_S^0$  mesons produced in p+p and p+ $\bar{p}$  interactions. The solid, dashed and dotted lines indicate parameterizations obtained for whole, “low” and “high”  $m_T$  intervals, respectively.

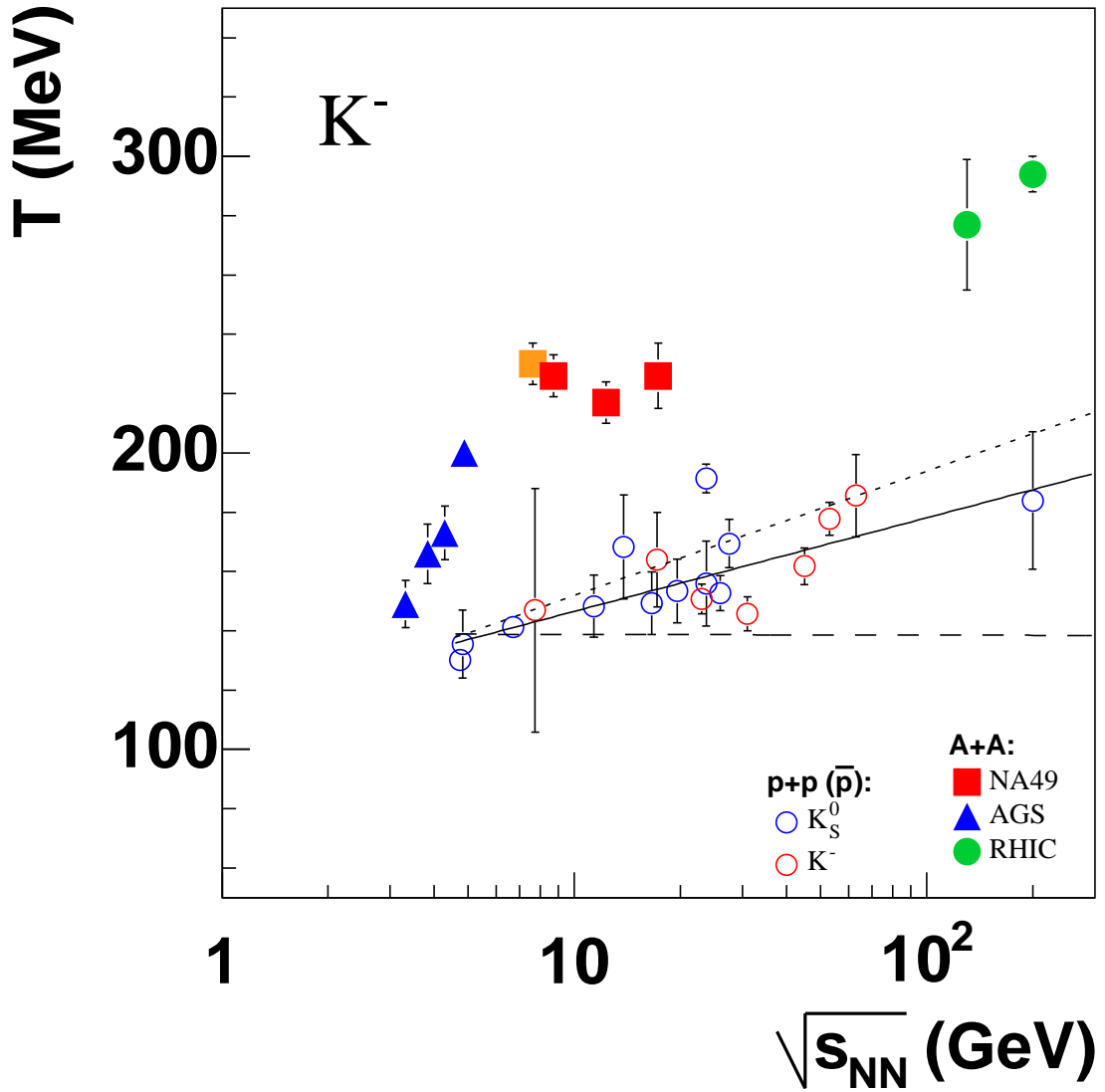


Figure 7: (Color online) Energy dependence of the inverse slope parameter  $T$  of transverse mass spectra of  $K^-$  mesons produced in central collisions of heavy nuclei (Pb+Pb [1, 2], Au+Au [12, 13, 14]) as well as  $K^-$  and  $K_S^0$  mesons produced in p+p and p+ $\bar{p}$  interactions. The solid, dashed and dotted lines indicate parameterizations obtained for whole, “low” and “high”  $m_T$  intervals, respectively.